HHS Public Access

Author manuscript

Clin Cancer Res. Author manuscript; available in PMC 2017 September 15.

Published in final edited form as:

Clin Cancer Res. 2016 September 15; 22(18): 4698–4711. doi:10.1158/1078-0432.CCR-15-2827.

A synthetic cell-penetrating dominant-negative ATF5 peptide exerts anti-cancer activity against a broad spectrum of treatment resistant cancers

Georg Karpel-Massler[1], **Basil A. Horst**[2], **Chang Shu**[1], **Lily Chau**[1], **Takashi Tsujiuchi**[3], **Jeffrey N. Bruce**[3], **Peter Canoll**[1], **Lloyd A. Greene**[1], **James M. Angelastro**[4], and **Markus D. Siegelin**[1]

[1] Department of Pathology & Cell Biology, Columbia University Medical Center, New York, New York, U.S.A.

[2] Department of Dermatology, Columbia University Medical Center, New York, New York, U.S.A.

[3] Department of Neurosurgery, Columbia University Medical Center, New York, New York, U.S.A.

[4] Department of Molecular Biosciences, University of California, Davis School of Veterinary Medicine, Davis, California, U.S.A.

Abstract

Purpose—Despite significant progress in cancer research many tumor entities still have an unfavorable prognosis. Activating Transcription Factor 5 (ATF5) is up-regulated in various malignancies and promotes apoptotic resistance. We evaluated the efficacy and mechanisms of the first described synthetic cell-penetrating inhibitor of ATF5 function, CP-d/n-ATF5-S1.

Experimental Design—Preclinical drug testing was performed in various treatment-resistant cancer cells and *in vivo* xenograft models.

Results—CP-d/n-ATF5-S1 reduced the transcript levels of several known direct ATF5 targets. It depleted endogenous ATF5 and induced apoptosis across a broad panel of treatment refractory cancer cell lines, sparing non-neoplastic cells. CP-d/n-ATF5-S1 promoted tumor cell apoptotic susceptibility in part by reducing expression of the deubiquitinase Usp9X and lead to diminished levels of anti-apoptotic Bcl-2 family members Mcl-1 and Bcl-2. In line with this, CP-d/n-ATF5-S1 synergistically enhanced tumor cell apoptosis induced by the BH3-mimetic ABT263 and the death ligand TRAIL. *In vivo,* CP-d/n-ATF5-S1 attenuated tumor growth as a single compound in

Correspondence to: Markus D. Siegelin, MD, Dr. med., Department of Pathology & Cell Biology, Columbia University Medical Center, 630 West 168th Street, P&S Rm. 15-401, New York, NY 10032, ms4169@cumc.columbia.edu, Phone: 212- 305-1993, James M. Angelastro, PhD, Department of Molecular Biosciences, University of California, One Shields Ave, Davis, CA 95616, jmangelastro@ucdavis.com, Phone: 530-752-1591.
Lily Chau's present address is: Department of Neurology, SUNY Downstate Medical Center, Brooklyn, New York, U.S.A.

Conflict of interests:
Columbia University, on behalf of inventors Drs. Angelastro and Greene, has been awarded United States patents US 07888326 "Methods for promoting apoptosis and treating tumor cells by inhibiting the expression or function of the transcription factor ATF5" and US 08158420 "Methods for inhibiting the differentiation of proliferative telencephalic cells in vitro by addition of ATF5". Columbia University/University of California, Davis; Provisional patent application was filed, February 22, 2013 with U.S. Provisional Application Serial No. 61/768,390. "Compositions and Methods for Inhibiting Tumor Cells by Inhibiting the Transcription Factor ATF5."
GKM, BAH, CS, LC, TT, JNB, PC and MDS declare no conflict of interest.

melanoma, glioblastoma, prostate cancer and triple-receptor-negative breast cancer xenograft models. Finally, the combination treatment of CP-d/n-ATF5-S1 and ABT263 significantly reduced tumor growth *in vivo* more efficiently than each reagent on its own.

Conclusions—Our data support the idea that CP-d/n-ATF5-S1, administered as a single reagent or in combination with other drugs, holds promise as an innovative, safe and efficient anti-neoplastic agent against treatment-resistant cancers.

Keywords

ATF5; cell-penetrating peptide; apoptosis; Usp9X; ABT263

Introduction

While recent significant responses for cancer therapy have been achieved in some malignancies, these are often initially impressive, but unfortunately not durable (1,2). For other malignancies, such as high-grade primary brain cancers the prognosis is unfavorable even with treatment (3). Therefore, efforts continue to identify new potential targets for tumor-specific treatments as well as novel therapeutic strategies to exploit these targets.

ATF5 is an example that has been identified as a potential target for cancer treatment but for which no specific therapy has been developed (4,5). Activating transcription factor 5 (ATF5; also termed ATFx), is a member of the activating transcription factor/cyclic AMP responsive element-binding (ATF/CREB) family. A common feature of this family is the presence of a basic leucine zipper (bZIP) domain that promotes DNA binding via the basic region and interactions with other proteins through the leucine zipper (5-7). ATF5 binds to several different promoter elements including the nutrient sensing report element (NRSE) and a novel motif to regulate gene transcription (6,8). Full length ATF5 appears to be rapidly degraded via the proteasome and it has the unusual property that it is among a small group of proteins that are selectively translated when eiF2α is phosphorylated (9,10).

ATF5 protein levels are increased in a variety of human malignancies, including glioblastoma, breast, pancreatic, lung and colon cancers (11). In contrast, with few exceptions (liver, prostate and testis) ATF5 expression is low in normal tissue of the respective organs. In several tumor types, including glioblastoma and non-small cell lung cancer, ATF5 expression negatively correlates with survival (12,13). In cell culture studies, ATF5 promotes survival by counteracting apoptosis in pro-B lymphocytes deprived of IL-3 or in HeLa cells after growth factor withdrawal (14). In addition, ATF5 regulates transcription of anti-apoptotic B cell leukemia 2 (Bcl-2) and of Bcl-2 family member, myeloid cell leukemia-1 (Mcl-1), presumably thereby promoting tumor cell survival (13,15). Conversely, interference with ATF5 expression or activity yields a marked induction of apoptosis in glioblastoma cells *in vitro* and *in vivo* without affecting astrocytes (16,17). Moreover, in a transgenic murine model in which endogenous glioblastomas were induced by a PDGF/sh-p53 expressing virus, activation of a dominant/negative (d/n)-ATF5 blocked tumor formation and resulted in regression of formed tumors (17). Antineoplastic activity of d/n-ATF5 was also reported for breast cancer cells and pancreatic cancer cells *in vitro*

(11,15,18). These findings thus suggest ATF5 as a promising target for a tailored anti-cancer therapy.

To provide a potential means to target ATF5 *in vivo*, we designed a d/n-ATF5 linked to a cell penetrating domain (Penetratin) (19). This recombinant peptide passes the blood brain barrier, enters tumor cells and exerts antineoplastic activity in a rodent transgenic glioma model. In the present study, we assessed the activity and mechanism of action of a similar peptide (CP-d/n-ATF5-S1) that was further modified to reduce its size and that was generated synthetically. In *in vitro* studies and in *in vivo* murine xenograft models, CP-d/n-ATF5-S1 shows apoptosis induction over a broad range of recalcitrant human malignancies without apparent effects on non-transformed cells. A novel mechanism of action was found in which the peptide reduces expression of the deubiquitinating enzyme Usp9X, which in turn leads to depletion of Mcl-1 and Bcl-2 and to consequent apoptotic death. The latter findings led us to rationally design and carry out *in vitro* and *in vivo* tests of several potential combination therapies with CP-d/n-ATF5-S1 that had enhanced efficacy compared with either agent alone.

Materials and Methods

Ethics statement

All procedures were in accordance with Animal Welfare Regulations and approved by the Institutional Animal Care and Use Committee at Columbia University Medical Center.

Reagents

CP-d/n-ATF5-S1, mutated CP-d/n-ATF5-S1 and Penetratin were purchased from CS Bio (Menlo Park, CA). Recombinant TRAIL was from Peprotech (Rocky Hill, NJ). ABT263 was from Selleckchem (Houston, TX).

Cell culture

Cells were grown as described (20,21). Cells were obtained from the ATCC or Cell Line Services and authenticated by the provider. No cell line authentication was performed by the authors and details are found in the supplementary section.

Cell viability assays

To examine cellular proliferation, 3-[4, 5-dimethylthiazol-2-yl]-2, 5-diphenyltetrazolium bromide (MTT) assays were performed as previously described (21).

Measurement of apoptosis and mitochondrial membrane potential

Annexin V/PI, PI and JC-1 stainings were performed as previously described (20,22).

Western blot analysis

Protein expression was determined by Western blot analysis as described before (23).

Transfections of siRNAs

siRNAs were transfected as described (22,24).

cDNA synthesis and Real-time PCR

cDNA synthesis and RT-PCR were performed as described before (23).

Subcutaneous xenograft models

Subcutaneous xenografts were implanted as previously described (20).

Statistical analysis

Statistical significance was assessed by Student's t-test using Prism version 5.04 (GraphPad, La Jolla, CA). A $p \leq 0.05$ was considered statistically significant.

Results

CP-d/n-ATF5-S1

CP-d/n-ATF5-S1 is a synthetic 67-amino-acid peptide that was engineered to cross cellular membranes and to specifically interfere with the survival-promoting actions of ATF5 (Figure 1A). The N-terminal has a 16 amino acid Penetratin domain that facilitates cellular penetration (25,26). A dominant/negative-sequence follows in which the DNA binding domain of ATF5 is substituted by an amphipathic sequence with a leucine repeat at every seventh residue and then by the human ATF5 basic leucine zipper (bZIP) domain truncated after the first valine (26-29). Parallel work has demonstrated that a similar recombinant tagged peptide passes the blood brain barrier, enters intact cells both *in vivo* and *in vitro* and promotes selective death of glioma cells (19). Four independent batches of the peptide (including one under GMP conditions) have had comparable activity. For control purposes, peptides were also synthesized with a penetratin domain alone and in which key leucine residues were mutated to glycine in the d/n portion to reduce binding to potential partners (Figure 1A)

CP-d/n-ATF5-S1 depletes endogenous ATF5

Western blot analyses revealed that treatment of cultured tumor cell lines (T98G, MDA-MB-436 and GBM12) with CP-d/n-ATF5-S1 leads to a dose-dependent reduction of endogenous ATF5 protein levels by 3 days (Figure 1B, Suppl. fig. 1B). In T98G cells this effect was present after 48, but not 24h (Figure 1B, Suppl. fig. 1A). RNAseq analysis of T98G glioblastoma cells treated with CP-d/n-ATF5-S1 for 1-3 days showed no significant alteration of ATF5 transcript levels (data not shown). Comparison of endogenous ATF5 levels in T98G cells treated with or without CP-d/n-ATF5-S1 in presence of cycloheximide indicates that the peptide significantly decreases ATF5 protein stability (Figure 1C and 1D, Suppl. fig. 1C). In contrast, treatment with Penetratin peptide did not affect ATF5 stability (Suppl. fig. 1D and 1E). Thus, one action of CP-d/n-ATF5-S1 is loss of endogenous ATF5 caused at least in part by enhanced turnover.

CP-d/n-ATF5-S1 interferes with transcription of known ATF5 downstream targets

CP-d/n-ATF5-S1 treatment for 24h resulted in down-regulation of three known ATF5 target genes (Mcl-1 (13), Bcl-2 (15,30) and asparagine synthetase (8)) at the mRNA-level (Figure 1E, Suppl. fig. 2). However, for Mcl-1 and Bcl-2, this decrease was transitory with mRNA levels returning to baseline by 72h, presumably by compensatory mechanisms. In contrast, CP-d/n-ATF5-S1 did not decrease mRNA levels of Usp9X, a gene not described as transcriptionally regulated by ATF5 (Figure 1E).

CP-d/n-ATF5-S1 promotes apoptotic cell death across a wide panel of treatment-resistant human cancer cell lines

ATF5 is expressed in a variety of human cancers including glioblastoma (11,15,18). *In silico* analysis of the Rembrandt data set for glioblastoma shows a significantly worse overall survival in patients harboring an amplification of the ATF5 gene compared with those with ≤ 1.8 copies (Figure 1F). Several studies have also reported an inverse relationship between ATF5 protein expression and GBM patient survival (5).

Inhibition of ATF5 function or expression has marked anti-neoplastic effects *in vitro* and *in vivo* (11,15,16,18). Initially, to assess the activity of CP-d/n-ATF5-S1, T98G, U87MG glioblastoma and HL-60 myeloid leukemia cells were treated for 72h with increasing concentrations of the peptide. CP-d/n-ATF5-S1 yielded a dose-dependent anti-proliferative effect as determined by MTT assay (Figure 1G and Suppl. fig. 3) as well as marked changes in cellular morphology observed by light microscopy (Figure 1H). To further assess the mechanism of such effects, we performed annexin V/PI staining across a variety of therapy-refractory human cancer cell lines after treatment with increasing concentrations of CP-d/n-ATF5-S1 for 48h. As shown in Figure 2A-C, Suppl. fig. 4A and 4C and Suppl. fig. 5A, the peptide yielded a strong and dose-dependent increase in the fraction of annexin V-positive cells, thus indicating an apoptotic response across a wide and diverse panel of solid and non-solid cancer cells. Moreover, this effect was attenuated by treatment with the pan-caspase inhibitor z-VAD-Fmk in T98G cells (Suppl. fig. 6), which is consistent with studies indicating that interference with ATF5 function or expression in tumor cells promotes apoptosis (9,12).

To verify whether the effect of the peptide on survival is specifically related to the dominant-negative domain and not to the cell-penetrating domain, we treated T98G cells either with Penetratin alone or CP-d/n-ATF5-S1. In contrast to CP-d/n-ATF5-S1, Penetratin did not markedly increase the fraction of annexin V-positive cells (Figure 2D and E). Moreover, neither Penetratin nor CP-d/n-ATF5-S1 resulted in a significant induction of apoptosis in human fetal astrocyte cultures (Figure 1F and G), suggesting that CP-d/n-ATF5-S1 posseses specificity towards cancer cells.

CP-d/n-ATF5-S1 leads to dissipation of mitochondrial membrane potential and activates caspase-9

Next, we addressed whether activation of apoptosis by CP-d/n-ATF5-S1 is mediated at least in part through a mitochondrial pathway. JC1 staining revealed that peptide treatment leads to a marked reduction of mitochondrial membrane potential (Figure 2H) and cleavage

(activation) of caspase-9, suggesting that CP-d/n-ATF5-S1 induces apoptosis in part through the mitochondrially-driven apoptotic pathway (Figure 2I).

CP-d/n-ATF5-S1 down-regulates anti-apoptotic Bcl-2 and Mcl-1 proteins

Because our findings pointed towards involvement of mitochondria in apoptosis driven by CP-d/n-ATF5-S1, we next focused on expression of Bcl-2 family proteins. ATF5 is reported to suppress transcription of anti-apoptotic Bcl-2 and Mcl-1 (13,30). However, at least in T98G cells, there was a rebound of Mcl-1 and Bcl-2 mRNA expression by 3 days of peptide treatment (Figure 1E), so it was important to assess protein levels at this time as well. As shown in Figure 3A and Suppl. fig. 7A, Mcl-1 was consistently down-regulated in all lines tested (U87MG, T98G glioblastoma and H1975 non-small cell lung cancer, PANC-1 pancreatic carcinoma, A375 melanoma and PC3 prostate cancer) at 72h of peptide treatment and in some cases, by 48h. Bcl-2 protein was similarly down-regulated in all but the PC3 cell line. Expression of Bcl-xL, a third member of the anti-apoptotic Bcl-2 family, was altered in some lines (U87MG and T98G), but not in others. Despite a rebound of Mcl-1 and Bcl-2 mRNA levels in T98G cells by 3 days of CP-d/n-ATF5-S1 treatment, expression of the corresponding protein was still decreased in these cells after 6 days of peptide treatment (Suppl. fig. 1F)

CP-d/n-ATF5-S1 down regulates Bag3 and Usp9X proteins

The observed decreases in Mcl-1 and Bcl-2 proteins at 72h promoted by CP-d/n-ATF5-S1 under conditions in which mRNA levels appear to be unaffected led us to next assess whether the peptide affects expression of Bcl-2 family members by a post-transcriptional mechanism. For instance, Mcl-1 is stabilized by its chaperone Bcl-2-associated athanogene 3 (Bag3) on one hand and by deubiquitination through the ubiquitin-specific peptidase 9, X-linked (Usp9X) on the other (31,32). Therefore, we determined protein levels of Bag3 and Usp9X in a panel of tumor lines following treatment with increasing concentrations of CP-d/n-ATF5-S1 for 48-72h. Usp9X expression was greatly reduced by peptide treatment in a time- and dose-dependent manner, while Bag3 levels fell particularly in U87MG, T98G and PC3 cells (Figure 3A, Suppl. fig. 7A and 7B). CP-d/n-ATF5-S1-mediated reduction in Usp9X protein levels was not rescued by z-VAD-fmk, indicating that Usp9X depletion is most likely independent of apoptosis and activated caspases as well as of its mRNA levels (Suppl. fig. 8 and Figure 1E).

Usp9X knockdown induces apoptosis, caspase activation and recapitulates effects of CP-d/n-ATF5-S1

The consistent effect of CP-d/n-ATF5-S1 on Usp9X expression led us to examine whether silencing Usp9X by another means would be sufficient to phenocopy the pro-apoptotic effect of the peptide. Similarly to cells treated with CP-d/n-ATF5-S1, T98G, U251 and LN229 glioblastoma cells in which Usp9X was silenced with siRNA showed marked reduction in viability as indicated by annexin V/PI or propidium iodide staining (Figure 3B, Suppl. fig. 9A). This was accompanied by a substantial increase in cleavage of caspases-9 and -3 (Figure 3C, Suppl. fig. 9B). Additionally, there was significant reduction in Bag3, Mcl-1 and Bcl-2 protein expression in both U251 and T98G cells. Taken together these findings

indicate that loss of Usp9X expression promoted by CP-d/n-ATF5-S1 treatment is sufficient to diminish levels of key anti-apoptotic Bcl-2 family members and to induce cell death.

CP-d/n-ATF5-S1 sensitizes for apoptosis induced by BH3-mimetics

Mcl-1 is a major resistance factor towards BH3-mimetics such as ABT737/263/199, and a considerable number of solid malignant tumors, including gliomas, bear high levels of Mcl-1 (33,34). Given that CP-d/n-ATF5-S1 modulates anti-apoptotic members of the Bcl-2 family, especially Mcl-1 and its interacting proteins, we examined whether the peptide may act in a complementary or synergistic fashion with BH3-mimetic agents. We accordingly treated T98G cells with CP-d/n-ATF5-S1 and Bcl-2/Bcl-xL inhibitor ABT263 or the Bcl-2/Bcl-xL/Mcl-1 inhibitor GX15-070. In both instances, combined treatment caused synergistic inhibition of cell viability as assessed by MTT assay (Figure 4A, Suppl. fig. 10A). In concordance, cellular morphology was markedly changed in cells subjected to the combination treatments and pointed, as anticipated, towards apoptosis as the underlying mechanism. (Figure 4B). Because GX15-070 has activities in addition to Bcl-2 family inhibition (35), we focused further combinatorial studies on ABT263. Enhancement of ABT263-mediated apoptosis by CP-d/n-ATF5-S1 was confirmed by annexin V/PI staining. The combination treatment significantly up-regulated the fraction of annexin V-positive cells in T98G, LN229, SF188 (pediatric), NCH644 (glioma stem-like) and GBM12 glioblastoma cultures as well as in PANC-1 pancreatic carcinoma, A375 melanoma, K562 chronic myeloid leukemia (in blast crisis) and HCT116 colorectal cancer cell cultures (Figure 4C and E, Suppl. fig. 5B and Suppl. fig. 11). Consistent with these findings, combined treatment with CP-d/n-ATF5-S1 and ABT263 also enhanced caspase-9 cleavage in T98G cells (Figure 4F).

In the context of these experiments, we also assessed a Penetratin-only peptide and a form of CP-d/n-ATF5-S1 mutated in the extended leucine zipper (Figure 1A) to diminish its interaction with other proteins. In comparison with CP-d/n-ATF5-S1, the mutated peptide showed markedly less effect on T98G cell morphology either alone or in combination with ABT263 (Figure 4B). The mutated peptide also showed much less effect on apoptosis when applied alone and minimally enhanced apoptosis when combined with the BH3-mimetic (Figure 4D). Moreover, combined treatment with the Penetratin peptide and ABT263 resulted in an antagonistic antiproliferative effect (Suppl. fig. 10B).

Combined CP-d/n-ATF5-S1 and ABT263 treatment promotes enhanced down-regulation of Mcl-1 and Bcl-2 which in turn results in enhanced apoptotic death

We next examined the effect of combined treatment with CP-d/n-ATF5-S1 and ABT263 on expression of anti-apoptotic Bcl-2 family members. As illustrated in Figure 4F, ABT263 alone increased expression of Mcl-1 – a finding that represents a generally accepted mechanism of resistance to BH3-mimetic compounds (34). However when ABT263 was combined with CP-d/n-ATF5-S1, Mcl-1 expression was highly suppressed, as was expression of Bcl-2 and Bcl-xL (Figure 4F). In contrast, combined treatment with ABT263 and mutated CP-d/n-ATF5-S1 yielded only a slight decrease in Mcl-1 and Bcl-2 expression (Figure 4F).

Part of the rationale for combining CP-d/n-ATF5-S1 with ABT263 is that unlike the latter, the former promotes Mcl-1 down-regulation. To examine whether down-regulation of Mcl-1, as occurs with CP-d/n-ATF5-S1, is sufficient to sensitize for ABT263-mediated apoptosis, we silenced Mcl-1 in PANC-1 cells with siRNA prior to treatment with ABT263 (Suppl. fig. 12A). Mcl-1 knock-down combined with ABT263 yielded markedly enhanced cleavage of caspases-9 and -3. Additionally, Bag3, Usp9X and Bcl-2 expression was significantly reduced under these conditions compared with cells either silenced for Mcl-1 and/or treated with ABT263 alone. These observations were also reflected by an enhanced reduction in the fraction of viable LN229 cells remaining after silencing Mcl-1 and treating with ABT263, as compared to treating with either alone (Suppl. fig. 12B). Similarly, when Usp9X was silenced, LN229 cells became more susceptible to the cytotoxic effects of ABT263 (Suppl. fig. 12C).

Thus, when combined with ABT263, specific knock-down of Mcl-1 and Usp9X (as seen after treatment with CP-d/n-ATF5-S1) suffices to reproduce the molecular profile of combined treatment with CP-d/n-ATF5-S1 and ABT263.

CP-d/n-ATF5-S1 enhances apoptosis induced by the death receptor ligand TRAIL

Next, we examined whether combined treatment with CP-d/n-ATF5-S1 also enhances apoptosis triggered by the extrinsic pathway. Our reasoning was that if the peptide increases sensitivity to the mitochondrial apoptotic pathway, it might complement or enhance mitochondrial-dependent and/or -independent apoptotic actions of a death-promoting ligand. We therefore treated T98G cells with CP-d/n-ATF5-S1 and increasing concentrations of TNF-related apoptosis-inducing ligand (TRAIL). As shown in Figure 5A, treatment with this combination results in an enhanced anti-proliferative effect in the MTT assay compared to control or single treatments. In contrast, the combination of TRAIL with mutated CP-d/n-ATF5-S1 did not show this effect. Representative microphotographs in Figure 5B illustrate these findings at the level of morphology. Annexin V/PI staining also showed that CP-d/n-ATF5-S1 enhances TRAIL-mediated apoptosis in T98G cells as well as in LN229 glioblastoma cells and MDA-MB-436 breast cancer cells (Figure 5C and E). In this assay, mutated CP-d/n-ATF5-S1 alone only slightly increased apoptotic cells when compared to controls and did not enhance TRAIL-induced apoptosis (Figure 5D). In concordance with these findings, the combination therapy led to reduced expression of full length caspase-3 in T98G cells, presumably due to elevated cleavage of this protein (Figure 5F). Mutated CP-d/n-ATF5-S1 did not have this effect. In addition, combined treatment with CP-d/n-ATF5-S1 and TRAIL enhanced down-regulation of Mcl-1 and Bcl-2 expression (Figure 5F). Treatment with TRAIL alone in this cell line reduced expression of Bcl-xL, though this effect was neither matched nor enhanced by CP-d/n-ATF5-S1 (Figure 5F).

CP-d/n-ATF5-S1 sensitizes for TRAIL-mediated apoptosis at least in part by down-regulating Bag3 and Mcl-1

Decreased expression of Mcl-1 following treatment with CP-d/n-ATF5-S1 represents a mechanism likely to contribute to the CP-d/n-ATF5-S1-mediated sensitization towards TRAIL. Because Bag3 stabilizes Mcl-1 (23) and our data indicate that CP-d/n-ATF5-S1 down-regulates Bag3 in most cell lines tested (Figure 5G), we examined whether Bag3

knock-down would phenocopy the sensitizing effect of CP-d/n-ATF5-S1 towards TRAIL. Silencing Bag3 in LN229 glioblastoma cells results in down-regulation of Mcl-1 (Figure 5G). When combined with TRAIL, Bag3 knock-down markedly increased cleavage of caspases-9 and -3. Consistent with these observations, treatment with Bag3-siRNA and TRAIL yields a significant increase in apoptosis of LN229 cells as determined by annexin V/PI staining (Figure 5H). Moreover, TRAIL combined with silencing of Mcl-1 with siRNA also markedly increased cleavage of caspases-9 and -3 and apoptosis in LN229 cells (Figure 5I and J). In contrast, Bag3 and Usp9X levels were not affected by Mcl-1 knock-down alone or when combined with TRAIL (Figure 5I). Taken together, these findings indicate that CP-d/n-ATF5-S1 sensitizes tumor cells to TRAIL and that this occurs at least in part by loss of Mcl-1 due to reduction of Bag3 expression.

CP-d/n-ATF5-S1 significantly attenuates tumor growth *in vivo*

We next assessed the therapeutic efficacy of CP-d/n-ATF5-S1 in multiple murine xenograft models. U87MG glioblastoma, A375 melanoma, PC3 prostate cancer cells, PANC-1 pancreatic cancer cells and HCT116 colorectal cancer cells were implanted subcutaneously; MDA-MB-231 triple-negative breast cancer cells were implanted in the mammary fat pad; and GBM12 patient-derived xenografts were implanted intracranially. Once tumors formed, mice were randomized and treated with CP-d/n-ATF5-S1, vehicle or penetratin peptide as outlined in Figure 6A-C, Suppl. fig. 5C, Suppl. fig. 13 and Suppl. fig. 14. Under these conditions, except for the cases of PANC-1 cells ($p=0.25$) and HCT116 cells ($p=0.18$), in all tumor types animals that received treatment with CP-d/n-ATF5-S1 had significantly smaller tumors than the animals treated with vehicle or Penetratin (Figure 6B,C; Suppl. fig. 5C, Suppl. fig. 13 and Suppl. fig. 14). Moreover, in a GBM12 intracranial patient-derived xenograft model, animals treated with CP-d/n-ATF5-S1 showed a median survival of 38 days which was significantly prolonged compared to 22.5 days in animals receiving vehicle (Figure 6A). While the treatments used here affected tumor growth rate, for the most part, they did not result in statistically significant regression of tumors. However, there was a statistically significant tumor regression in mice bearing MDA-MB-231 breast cancer mammary fat pad xenografts (Suppl. fig. 14E-G). This effect was not observed when mice were treated with Penetratin alone (Suppl. fig. 14E-G).

To detect possible toxic effects due to peptide treatment, histological analysis was performed on various tumor-free tissues of animals treated with either vehicle or CP-d/n-ATF5-S1 according to the dosing schedule described in Figure 6C. No tissue alterations in brain, lung, kidney, heart, liver, spleen, and intestine were found (Suppl. fig. 15A). Moreover, the body weights of the animals did not vary between the treatment groups toward the end of the experiment (Suppl. fig. 15B).

Combined treatment with CP-d/n-ATF5-S1 and ABT263 significantly enhances attenuation of tumor growth *in vivo*

Our *in vitro* studies indicated that combined CP-d/n-ATF5-S1 and ABT263 treatment enhanced tumor cell death due to additive and complementary effects on anti-apoptotic Bcl-2 family members. To assess whether the combination is more effective *in vivo* than either treatment alone, we utilized a U251 heterotopic glioblastoma xenograft model and a

HCT116 heterotopic colorectal cancer xenograft model Figure 6D and Suppl. fig. 5C. The mice with xenografted tumors were divided into four groups: vehicle, ABT263, CP-d/n-ATF5-S1 or the combination of ABT263 and CP-d/n-ATF5-S1. As shown in Figure 6D, in the U251 model, at the end point of the study, animals that received the combination treatment had significantly smaller tumors compared to those treated either with ABT263 or CP-d/n-ATF5-S1 alone and showed a decrease in tumor size over time when compared to the beginning of treatment. Similarly, in the HCT116 model the combination treatment led to significant reduction in tumor growth rate when compared to vehicle or single-agent treatments (Suppl. fig. 5C). The combination treatment also showed no clinical signs of toxicity, indicating that although the combined treatment is more efficient, it does not increase the occurrence of evident side effects.

Discussion

Cancer cells typically develop primary or secondary resistance to apoptosis (36). Therefore, means to manipulate the apoptotic machinery are pivotal to restore therapeutic sensitivity. Deregulation of the apoptotic machinery is mediated through numerous factors, such as the Bcl-2 family of proteins, the Inhibitor of Apoptosis Proteins and expression of death receptors, initiator caspases and endogenous caspase inhibitors (37,38). The aberrant expression of such molecules is regulated by various means, including the actions of transcription factors. ATF5 is an example of a transcription factor with oncogenic potential that affects Bcl-2 family member expression (13,16). ATF5 is up-regulated in various malignancies, including highly prevalent tumors, such as breast carcinoma (11), but it is also increased in less common malignancies, such as low- and high-grade gliomas (13,16). In the context of low- and high-grade gliomas, ATF5 expression levels are not only increased, but also correlate with survival (13). Thus, ATF5 represents a potential target in treatment refractory cancers.

Here, we show that a novel synthetic cell penetrating dominant-negative ATF5 peptide induces apoptosis in a broad range of tumor types, including glioblastoma, triple-negative breast cancer (MDA-MB-436), hormone-refractory prostate cancer (PC3 and DU145), EGFR kinase inhibitor resistant non-small cell lung cancer (H1975), BRAF (V600E)-mutated melanoma (A375) and pancreatic carcinoma (PANC-1). CP-d/n-ATF5-S1 also showed *in vivo* efficacy in reducing growth of a range of tumor types in xenograft models. We have yet to optimize dosing or regimens of administration. Our *in vitro* and *in vivo* studies indicate that the peptide does not kill non-transformed cells and causes no evident histological or behavioral signs of toxicity in mice at levels up to at least 150 mg/kg. With respect to specificity, a Penetratin peptide and a peptide in which key leucine residues in CP-d/n-ATF5-S1 were mutated showed no or little apoptotic activity alone or in combination studies. The fact that ATF5, as a pro-survival factor is overexpressed in cancer cells, may cause a state of cellular ATF5-dependency in the sense of oncogene addiction. This would explain the selective response towards CP-d/n-ATF5-S1 treatment in cancer cells as a consequence of a sudden CP-d/n-ATF5-S1-mediated loss of ATF5 function.

CP-d/n-ATF5-S1-mediated cell death was accompanied by depletion of endogenous ATF5 protein suggesting that CP-d/n-ATF5-S1 may induce cell death in part through depletion of

total ATF5 levels. In that context, earlier results showed that depletion of ATF5 by siRNA/shRNA leads to cell death in a broad variety of tumor cells (11,13,15). It remains to be determined by what underlying mechanisms CP-d/n-ATF5-S1 controls ATF5 protein levels. Our observations suggest that this is a non-transcriptional event. Given that ATF5 possesses a short-half life (39) and is stabilized by chaperones (39), it is conceivable that CP-d/n-ATF5-S1 enhances ATF5's degradation through disruption of its interactions with other binding partners.

Consistent with its activation of the intrinsic apoptotic pathway, CP-d/n-ATF5-S1 modulated the expression of the anti-apoptotic Bcl-2 protein family, including Mcl-1, Bcl-2 and, in some instances, Bcl-xL. Particularly at earlier time points, there is an occasional CP-d/n-ATF5-mediated increase in Bcl-xL, which, however, for most cell lines (except for PANC1) tested is not sustained. Additional research will shed light on why CP-d/n-ATF5-S1 causes this biphasic modulation of Bcl-xL. Nevertheless, one possible consequence might be that the increase in Bcl-xL might render tumor cells more sensitive to Bcl-xL inhibitors, such as ABT263. These are known to counteract Bax-dependent apoptosis by preventing mitochondrial outer membrane permeabilization and subsequent cytochrome-c release and caspase-9 activation.

Although Bcl-2 and Mcl-1 have been described as transcriptional targets of ATF5, our findings indicate that CP-d/n-ATF5-S1 causes only a transient decrease in their transcript levels and that Mcl-1, in particular, is subject to sustained down-regulation at the posttranscriptional level by CP-d/n-ATF5-S1. Several molecules have been described that control Mcl-1 levels posttranslationally. Examples include MULE (40), Bag3 (31) and Usp9X (32). Bag3 is a co-chaperone of Hsp70 (41) and binds Mcl-1 to prevent its degradation, while Usp9X is a deubiquitinase that removes ubiquitin chains from Mcl-1, rendering it resistant to proteasomal degradation and thereby in turn increasing its half-life (32). Both Bag3 and Usp9X have been shown to counteract intrinsic apoptosis. For instance, Bag3 is up-regulated in malignant gliomas and intereferes with Bax-mediated apoptosis (42) while Usp9X knockdown enhances ABT263-mediated cell death in glioblastoma (20,33). Usp9X interacts with a variety of molecules in addition to Bcl-2 proteins that may also affect cell survival (43,44) and these too may thus play a role in tumor cell death promoted by CP-d/n-ATF5-S1.

Our findings show that in PC3, PANC-1, T98G, H1975, A375 and U87MG cells, CP-d/n-ATF5-S1 significantly affects protein levels of Usp9X starting as early as 48h and continuing at 72h after treatment, when apoptotic death is manifest. To assess the impact of Usp9X depletion by CP-d/n-ATF5-S1, we transfected glioblastoma cells with Usp9X siRNA and found that this was sufficient to induce significant apoptotic death. Mechanistically, Usp9X knockdown caused concomitant suppression of Bag3, Mcl-1 and Bcl-2 expression, which remarkably recapitulates the effects of CP-d/n-ATF5-S1 on these molecules. These observations suggest that CP-d/n-ATF5-S1-mediated suppression of Usp9X levels may be an instrumental mechanism by which it mediates death of neoplastic cells. While Usp9X is known to modulate Mcl-1 expression, our observed effects of Usp9X manipulation on Bag3 and Bcl-2 have not been previously described and may suggest that Usp9X also interacts with Bag3 as well as Bcl-2. The mechanism(s) by which CP-d/n-ATF5-S1 decreases Usp9X

expression remain to be explored. Our data indicate a post-transcriptional mechanism in that the peptide does not affect Usp9X mRNA levels. The strong antineoplastic activity related to Usp9X down-regulation warrants further studies directed at identification of specific small-molecule inhibitors of Usp9X function.

Given our observation that CP-d/n-ATF5-S1 strongly affects the intrinsic apoptotic machinery and the possibility that treatment with a single drug may fall short in the clinic, we investigated whether rational drug combination therapies could enhance the efficacy of CP-d/n-ATF5-S1. For that purpose, we utilized the orally available BH3-mimetic ABT263 (43). This class of compounds has received great attention since they target both Bcl-2 and Bcl-xL, which are up-regulated in many malignancies, especially in hematological malignancies, such as follicular lymphoma (45), and also in solid neoplasms, such as glioblastoma (46). While certain tumors demonstrate remarkable sensitivity for BH3-mimetics, others reveal resistance, which in the vast majority of cases is attributed to high-levels of Mcl-1 expression (47). Therefore, means to counteract high Mcl-1 protein levels may sensitize resistant tumors to BH3-mimetic treatment (48,49). In the current case, we found that CP-d/n-ATF5-S1 strongly depresses expression of two Mcl-1 interacting proteins, Bag3 and Usp9X, and that this in turn leads to Mcl-1 depletion. These considerations led us to assess the combination of CP-d/n-ATF5-S1 and ABT263 *in vitro* and in *in vivo* xenograft tumor models. We found enhanced cell death by this combination in a variety of tumor cell lines, including LN229 and A375 that are relatively resistant to ABT263. In the *in vivo* models, the combination was highly effective compared with the single treatments and blocked/reduced tumor growth over the course of the studies.

Because the Bcl-2 family is also implicated in extrinsic apoptosis, we tested whether CP-d/n-ATF5-S1 overcomes resistance to TRAIL. TRAIL has received attention for its ability to kill a broad variety of cancer cells *in vitro* and *in vivo*. One main obstacle for TRAIL-related therapies is that while a subset of tumors respond, the majority display resistance (50). Therefore, efforts have aimed to identify treatments that sensitize cancer cells to TRAIL therapeutics. Our results suggest that CP-d/n-ATF5-S1 is a potent sensitizer for TRAIL-mediated apoptosis. Mechanistically this is most likely linked to the ability of CP-d/n-ATF5-S1 to suppress Bag3 and Mcl-1, since specific knockdown of Bag3 or Mcl-1 was sufficient to sensitize TRAIL-resistant LN229 glioblastoma cells to apoptosis.

Overall, our results serve as a proof of principle and suggest that the strategy of treatment with a cell penetrating dominant-negative form of ATF5 is efficacious, selective and non-toxic and therefore holds promise for cancer therapy, either alone or in a multi-targeting approach.

Supplementary Material

Refer to Web version on PubMed Central for supplementary material.

Acknowledgements

We thank Yanping Sun for excellent assistance with the MRI studies.

Financial support:

This work was supported by a scholarship from the Dr. Mildred Scheel foundation of the German Cancer Aid to GKM and American Brain Tumor Association, Translational Grant 2013 (ABTACU13-0098), the 2013 AACR-National Brain Tumor Society Career Development Award for Translational Brain Tumor Research (13-20-23-SIEG), NIH NINDS award K08NS083732 to MDS and NIH NINDS grant R01NS083795 to JMA and LAG.

References

1. Sosman JA, Kim KB, Schuchter L, Gonzalez R, Pavlick AC, Weber JS, et al. Survival in BRAF V600-mutant advanced melanoma treated with vemurafenib. N Engl J Med. 2012; 366(8):707–14. [PubMed: 22356324]
2. Tsao MS, Sakurada A, Cutz JC, Zhu CQ, Kamel-Reid S, Squire J, et al. Erlotinib in lung cancer - molecular and clinical predictors of outcome. N Engl J Med. 2005; 353(2):133–44. [PubMed: 16014883]
3. Stupp R, Mason WP, van den Bent MJ, Weller M, Fisher B, Taphoorn MJ, et al. Radiotherapy plus concomitant and adjuvant temozolomide for glioblastoma. N Engl J Med. 2005; 352(10):987–96. [PubMed: 15758009]
4. Greene LA, Lee HY, Angelastro JM. The transcription factor ATF5: role in neurodevelopment and neural tumors. J Neurochem. 2009; 108(1):11–22. [PubMed: 19046351]
5. Sheng Z, Evans SK, Green MR. An activating transcription factor 5-mediated survival pathway as a target for cancer therapy? Oncotarget. 2010; 1(6):457–60. [PubMed: 21311102]
6. Li G, Li W, Angelastro JM, Greene LA, Liu DX. Identification of a novel DNA binding site and a transcriptional target for activating transcription factor 5 in c6 glioma and mcf-7 breast cancer cells. Mol Cancer Res. 2009; 7(6):933–43. [PubMed: 19531563]
7. Vinson C, Acharya A, Taparowsky EJ. Deciphering B-ZIP transcription factor interactions in vitro and in vivo. Biochim Biophys Acta. 2006; 1759(1-2):4–12. [PubMed: 16580748]
8. Al Sarraj J, Vinson C, Thiel G. Regulation of asparagine synthetase gene transcription by the basic region leucine zipper transcription factors ATF5 and CHOP. Biol Chem. 2005; 386(9):873–9. [PubMed: 16164412]
9. Watatani Y, Ichikawa K, Nakanishi N, Fujimoto M, Takeda H, Kimura N, et al. Stress-induced translation of ATF5 mRNA is regulated by the 5'-untranslated region. J Biol Chem. 2008; 283(5): 2543–53. [PubMed: 18055463]
10. Zhou D, Palam LR, Jiang L, Narasimhan J, Staschke KA, Wek RC. Phosphorylation of eIF2 directs ATF5 translational control in response to diverse stress conditions. J Biol Chem. 2008; 283(11): 7064–73. [PubMed: 18195013]
11. Monaco SE, Angelastro JM, Szabolcs M, Greene LA. The transcription factor ATF5 is widely expressed in carcinomas, and interference with its function selectively kills neoplastic, but not nontransformed, breast cell lines. Int J Cancer. 2007; 120(9):1883–90. [PubMed: 17266024]
12. Ishihara S, Yasuda M, Ishizu A, Ishikawa M, Shirato H, Haga H. Activating transcription factor 5 enhances radioresistance and malignancy in cancer cells. Oncotarget. 2015; 6(7):4602–14. [PubMed: 25682872]
13. Sheng Z, Li L, Zhu LJ, Smith TW, Demers A, Ross AH, et al. A genome-wide RNA interference screen reveals an essential CREB3L2-ATF5-MCL1 survival pathway in malignant glioma with therapeutic implications. Nat Med. 2010; 16(6):671–7. [PubMed: 20495567]
14. Persengiev SP, Devireddy LR, Green MR. Inhibition of apoptosis by ATFx: a novel role for a member of the ATF/CREB family of mammalian bZIP transcription factors. Genes Dev. 2002; 16(14):1806–14. [PubMed: 12130540]
15. Chen A, Qian D, Wang B, Hu M, Lu J, Qi Y, et al. ATF5 is overexpressed in epithelial ovarian carcinomas and interference with its function increases apoptosis through the downregulation of Bcl-2 in SKOV-3 cells. Int J Gynecol Pathol. 2012; 31(6):532–7. [PubMed: 23018213]
16. Angelastro JM, Canoll PD, Kuo J, Weicker M, Costa A, Bruce JN, et al. Selective destruction of glioblastoma cells by interference with the activity or expression of ATF5. Oncogene. 2006; 25(6): 907–16. [PubMed: 16170340]

17. Arias A, Lame MW, Santarelli L, Hen R, Greene LA, Angelastro JM. Regulated ATF5 loss-of-function in adult mice blocks formation and causes regression/eradication of gliomas. Oncogene. 2012; 31(6):739–51. [PubMed: 21725368]
18. Hu M, Wang B, Qian D, Li L, Zhang L, Song X, et al. Interference with ATF5 function enhances the sensitivity of human pancreatic cancer cells to paclitaxel-induced apoptosis. Anticancer Res. 2012; 32(10):4385–94. [PubMed: 23060563]
19. Cates CC, Arias AD, Nakayama Wong LS, Lame MW, Sidorov M, Cayanan G, et al. Regression/eradication of gliomas in mice by a systemically-deliverable ATF5 dominant-negative peptide. Oncotarget. 2016 Epub ahead of print.
20. Karpel-Massler G, Ba M, Shu C, Halatsch ME, Westhoff MA, Bruce JN, et al. TIC10/ONC201 synergizes with Bcl-2/Bcl-xL inhibition in glioblastoma by suppression of Mcl-1 and its binding partners in vitro and in vivo. Oncotarget. 2015; 6(34):36456–71. [PubMed: 26474387]
21. Karpel-Massler G, Westhoff MA, Zhou S, Nonnenmacher L, Dwucet A, Kast RE, et al. Combined inhibition of HER1/EGFR and RAC1 results in a synergistic antiproliferative effect on established and primary cultured human glioblastoma cells. Mol Cancer Ther. 2013; 12(9):1783–95. [PubMed: 23832120]
22. Siegelin MD, Dohi T, Raskett CM, Orlowski GM, Powers CM, Gilbert CA, et al. Exploiting the mitochondrial unfolded protein response for cancer therapy in mice and human cells. J Clin Invest. 2011; 121(4):1349–60. [PubMed: 21364280]
23. Pareja F, Macleod D, Shu C, Crary JF, Canoll PD, Ross AH, et al. PI3K and Bcl-2 inhibition primes glioblastoma cells to apoptosis through downregulation of Mcl-1 and Phospho-BAD. Mol Cancer Res. 2014; 12(7):987–1001. [PubMed: 24757258]
24. Karpel-Massler G, Pareja F, Aime P, Shu C, Chau L, Westhoff MA, et al. PARP inhibition restores extrinsic apoptotic sensitivity in glioblastoma. PloS one. 2014; 9(12):e114583. [PubMed: 25531448]
25. Derossi D, Chassaing G, Prochiantz A. Trojan peptides: the penetratin system for intracellular delivery. Trends Cell Biol. 1998; 8(2):84–7. [PubMed: 9695814]
26. Greene, LA.; Angelastro, JM. Compositions and methods for inhibiting tumor cells by inhibiting the transcription factor ATF5. 2014.
27. Angelastro JM, Ignatova TN, Kukekov VG, Steindler DA, Stengren GB, Mendelsohn C, et al. Regulated expression of ATF5 is required for the progression of neural progenitor cells to neurons. J Neurosci. 2003; 23(11):4590–600. [PubMed: 12805299]
28. Moll JR, Olive M, Vinson C. Attractive interhelical electrostatic interactions in the proline- and acidic-rich region (PAR) leucine zipper subfamily preclude heterodimerization with other basic leucine zipper subfamilies. J Biol Chem. 2000; 275(44):34826–32. [PubMed: 10942764]
29. Vinson CR, Hai T, Boyd SM. Dimerization specificity of the leucine zipper-containing bZIP motif on DNA binding: prediction and rational design. Genes Dev. 1993; 7(6):1047–58. [PubMed: 8504929]
30. Dluzen D, Li G, Tacelosky D, Moreau M, Liu DX. BCL-2 is a downstream target of ATF5 that mediates the prosurvival function of ATF5 in a cell type-dependent manner. J Biol Chem. 2011; 286(9):7705–13. [PubMed: 21212266]
31. Boiani M, Daniel C, Liu X, Hogarty MD, Marnett LJ. The stress protein BAG3 stabilizes Mcl-1 protein and promotes survival of cancer cells and resistance to antagonist ABT-737. J Biol Chem. 2013; 288(10):6980–90. [PubMed: 23341456]
32. Schwickart M, Huang X, Lill JR, Liu J, Ferrando R, French DM, et al. Deubiquitinase USP9X stabilizes MCL1 and promotes tumour cell survival. Nature. 2010; 463(7277):103–7. [PubMed: 20023629]
33. Karpel-Massler G, Shu C, Chau L, Banu M, Halatsch ME, Westhoff MA, et al. Combined inhibition of Bcl-2/Bcl-xL and Usp9X/Bag3 overcomes apoptotic resistance in glioblastoma in vitro and in vivo. Oncotarget. 2015; 6(16):14507–21. [PubMed: 26008975]
34. Konopleva M, Contractor R, Tsao T, Samudio I, Ruvolo PP, Kitada S, et al. Mechanisms of apoptosis sensitivity and resistance to the BH3 mimetic ABT-737 in acute myeloid leukemia. Cancer Cell. 2006; 10(5):375–88. [PubMed: 17097560]

35. McCoy F, Hurwitz J, McTavish N, Paul I, Barnes C, O'Hagan B, et al. Obatoclax induces Atg7-dependent autophagy independent of beclin-1 and BAX/BAK. Cell Death Dis. 2010; 1:e108. [PubMed: 21368880]
36. Holohan C, Van Schaeybroeck S, Longley DB, Johnston PG. Cancer drug resistance: an evolving paradigm. Nat Rev Cancer. 2013; 13(10):714–26. [PubMed: 24060863]
37. Marini ES, Giampietri C, Petrungaro S, Conti S, Filippini A, Scorrano L, et al. The endogenous caspase-8 inhibitor c-FLIP regulates ER morphology and crosstalk with mitochondria. Cell Death Differ. 2014
38. Yip KW, Reed JC. Bcl-2 family proteins and cancer. Oncogene. 2008; 27(50):6398–406. [PubMed: 18955968]
39. Li G, Xu Y, Guan D, Liu Z, Liu DX. HSP70 protein promotes survival of C6 and U87 glioma cells by inhibition of ATF5 degradation. J Biol Chem. 2011; 286(23):20251–9. [PubMed: 21521685]
40. Zhong Q, Gao W, Du F, Wang X. Mule/ARF-BP1, a BH3-only E3 ubiquitin ligase, catalyzes the polyubiquitination of Mcl-1 and regulates apoptosis. Cell. 2005; 121(7):1085–95. [PubMed: 15989957]
41. Colvin TA, Gabai VL, Gong J, Calderwood SK, Li H, Gummuluru S, et al. Hsp70-Bag3 interactions regulate cancer-related signaling networks. Cancer Res. 2014; 74(17):4731–40. [PubMed: 24994713]
42. Festa M, Del Valle L, Khalili K, Franco R, Scognamiglio G, Graziano V, et al. BAG3 protein is overexpressed in human glioblastoma and is a potential target for therapy. The Am J Pathol. 2011; 178(6):2504–12. [PubMed: 21561597]
43. Tse C, Shoemaker AR, Adickes J, Anderson MG, Chen J, Jin S, et al. ABT-263: a potent and orally bioavailable Bcl-2 family inhibitor. Cancer res. 2008; 68(9):3421–8. [PubMed: 18451170]
44. Xie Y, Avello M, Schirle M, McWhinnie E, Feng Y, Bric-Furlong E, et al. Deubiquitinase FAM/USP9X interacts with the E3 ubiquitin ligase SMURF1 protein and protects it from ligase activity-dependent self-degradation. J Biol Chem. 2013; 288(5):2976–85. [PubMed: 23184937]
45. Mahadevan D, Fisher RI. Novel therapeutics for aggressive non-Hodgkin's lymphoma. J Clin Oncol. 2011; 29(14):1876–84. [PubMed: 21483007]
46. Cristofanon S, Fulda S. ABT-737 promotes tBid mitochondrial accumulation to enhance TRAIL-induced apoptosis in glioblastoma cells. Cell Death Dis. 2012; 3:e432. [PubMed: 23190604]
47. Lucas KM, Mohana-Kumaran N, Lau D, Zhang XD, Hersey P, Huang DC, et al. Modulation of NOXA and MCL-1 as a strategy for sensitizing melanoma cells to the BH3-mimetic ABT-737. Clin Cancer Res. 2012; 18(3):783–95. [PubMed: 22173547]
48. Preuss E, Hugle M, Reimann R, Schlecht M, Fulda S. Pan-mammalian target of rapamycin (mTOR) inhibitor AZD8055 primes rhabdomyosarcoma cells for ABT-737-induced apoptosis by down-regulating Mcl-1 protein. J Biol Chem. 2013; 288(49):35287–96. [PubMed: 24133218]
49. Vaillant F, Merino D, Lee L, Breslin K, Pal B, Ritchie ME, et al. Targeting BCL-2 with the BH3 mimetic ABT-199 in estrogen receptor-positive breast cancer. Cancer Cell. 2013; 24(1):120–9. [PubMed: 23845444]
50. Dimberg LY, Anderson CK, Camidge R, Behbakht K, Thorburn A, Ford HL. On the TRAIL to successful cancer therapy? Predicting and counteracting resistance against TRAIL-based therapeutics. Oncogene. 2013; 32(11):1341–50. [PubMed: 22580613]

Statement of translational relevance

Targeting treatment resistant malignancies remains a major challenge in oncology. In the present study, we introduce a novel therapeutic compound targeting Activating Transcription Factor 5 (ATF5) through utilization of a novel cell penetrating peptide, termed CP-d/n-ATF5-S1. CP-d/n-ATF5-S1 displays broad anti-cancer activity against glioblastoma, triple receptor negative breast cancer, prostatic carcinoma, pancreatic cancer, melanoma, non-small cell lung carcinoma and hematological malignancies. Notably, we provide evidence that these anti-neoplastic effects are not only observed *in vitro*, but are also seen in 6 different animal models of glioblastoma, melanoma, prostatic adenocarcinoma, triple-receptor negative breast cancer and pancreatic carcinoma without any detectable toxicity. Finally, CP-d/n-ATF5-S1 sensitizes tumor cells for BH3-mimetics and extrinsic apoptotic stimuli *in vitro* and *in vivo*. Taken together, CP-d/n-ATF5-S1 is a novel highly efficacious anti-cancer compound with minimal toxicity and potentially warrants clinical testing in patients.

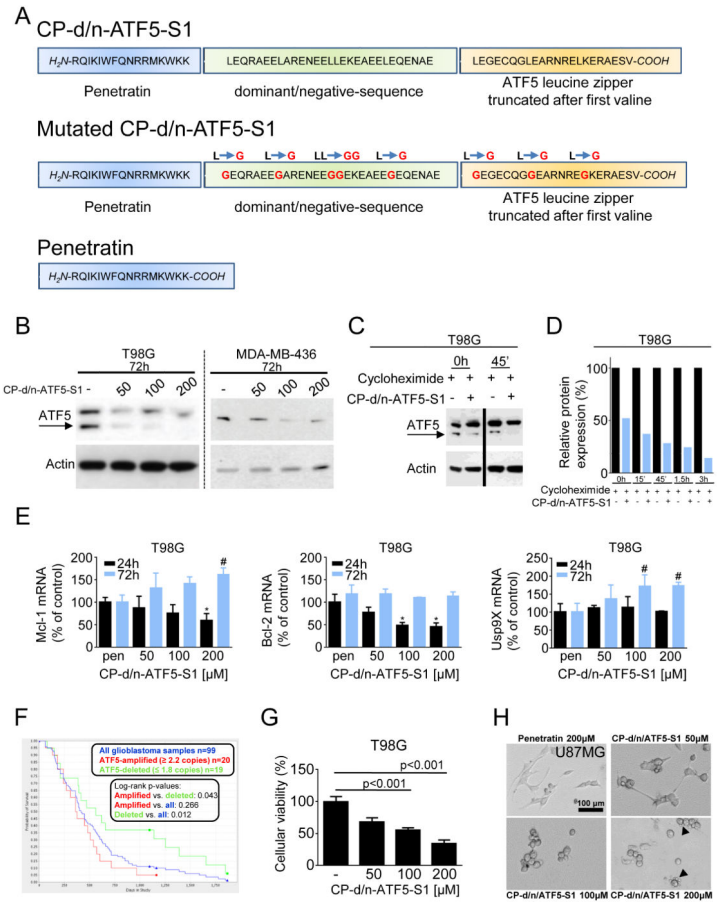

Figure 1.

A, Graphical representation showing the sequences of CP-d/n-ATF5-S1, Mutated CP-d/n-ATF5-S1 and Penetratin. B, T98G glioblastoma and MDA-MB-436 breast cancer cells were treated for 72h with increasing concentrations of CP-d/n-ATF5-S1 under reduced serum conditions to mimick the nutrient-deprived state of tumor cells in the tumor tissue (1.5% FBS) followed by Western blot analysis for ATF5. Actin Western blot analysis was performed to confirm equal protein loading. Arrow indicates the specific band of ATF5. C, T98G glioblastoma cells were treated with CP-d/n-ATF5-S1 or solvent for 48h prior to adding 10 μM cycloheximide and Western blot analysis for ATF5 and actin. D, Graphical representation following densitometric analysis of the experiment described under C using ImageJ (National Institutes of Health, U.S.A., http://imagej.nih.gov/ij). E, T98G glioblastoma cells were treated for the indicated durations with 100 μM Penetratin (pen) or increasing concentrations of CP-d/n-ATF5-S1 prior to performing rtqPCR for Mcl-1, Bcl-2 and Usp9X. Columns: Mean. Error bars: standard deviation. * signifies a p-value of less than 0.05 versus treatment with pen for 24h. # signifies a p-value of less than 0.05 versus treatment with pen for 72h. F, *In silico* analysis on the survival of glioblastoma patients based on the amplification status of the ATF5 gene (National Cancer Institute. 2005. REMBRANDT home page. <http://rembrandt.nci.nih.gov>. Accessed 2014 August 24). *G*, T98G glioblastoma cells were treated with increasing concentrations of CP-d/n-ATF5-S1 under low serum conditions (1.5% FBS). After 72h, a MTT assay was performed. Data

presented are representative for at least two independent experiments. Columns: means. Error bars: standard error of the mean (SEM). *H*, representative microphotographs of U87MG cells at 40x magnification after 72h of treatment with CP-d/n-ATF5-S1. Morphological changes such as decreased lengths and numbers of cell processes are especially seen in those cells treated with 200 μM CP-d/n-ATF5-S1. Black arrow tip points at blebs.

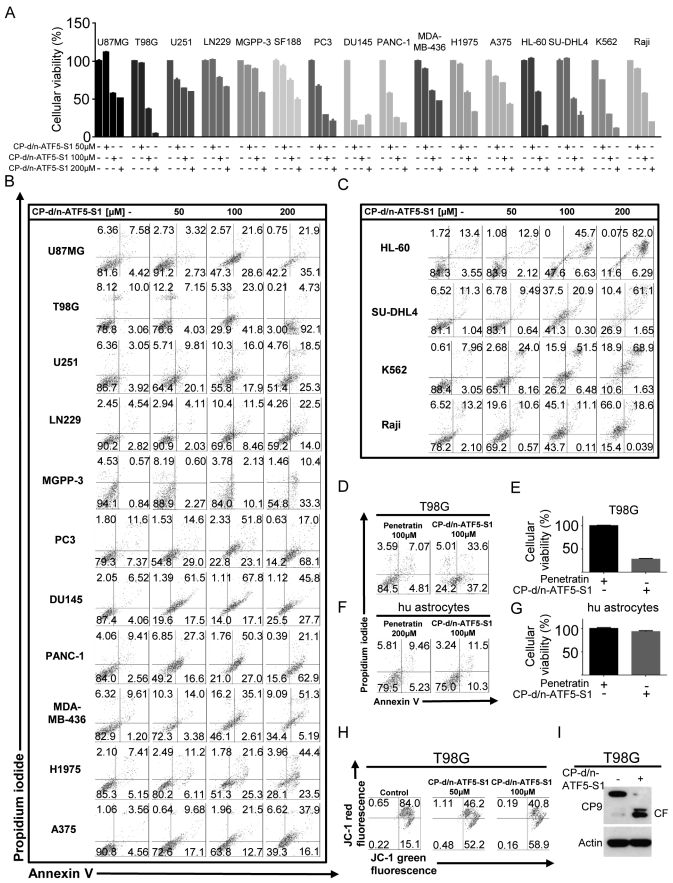

Figure 2.

A, U87MG, T98G, U251, LN229, MGPP-3 (transgenic, proneural) glioblastoma, PC3 and DU1145 prostate cancer, PANC-1 pancreatic carcinoma, MDA-MB-436 triple negative breast cancer, H1975 non-small cell lung cancer, A375 malignant melanoma HL-60 myeloid leukemia, SU-DHL4 diffuse large B-cell lymphoma, K562 chronic myeloid leukemia (in blast crisis) and Raji Burkitt lymphoma cells were treated for 48h with increasing concentrations of CP-d/n-ATF5-S1 prior to staining with annexin V/propidium iodide and flowcytometric analysis. Quantitative representation of the fraction of viable cells (annexin V and PI-negative cells). Columns, means of three serial measurements. Bars, SD. *B* and *C*, Representative flow plots of cells treated as described for *A*. Lower left quadrant, fraction of viable cells; upper left quadrant, fraction of necrotic cells; lower right quadrant, fraction of early apoptotic cells and upper right quadrant, fraction of late apoptotic cells. *D*, T98G glioblastoma cells were treated for 48h either with Penetratin or CP-d/n-ATF5-S1. Then staining for annexin V/PI was performed to detect apoptosis. *E*, Quantitative representation of cells treated as described for *D*. Columns, means of three serial measurements. Bars, SD. *F*, Human astrocytes were treated for 48h either with Penetratin or CP-d/n-ATF5-S1 and then staining for annexin V/PI was performed to detect apoptosis. *G*, Quantitative representation of cells treated as described for *D*. Columns, means of three serial measurements. Bars, SD. *H*, Representative flow plots of T98G glioblastoma cells that were treated for 48h with indicated concentrations of CP-d/n-ATF5-S1 prior to staining for JC-1 and flow cytometric analysis. *I*, T98G glioblastoma cells were treated for 6h with CP-d/n-

ATF5-S1 or control. Whole cell extracts were collected and Western blot for caspase-9 (CP9) and actin was performed. The cleaved form of caspase-9 is marked by CF.

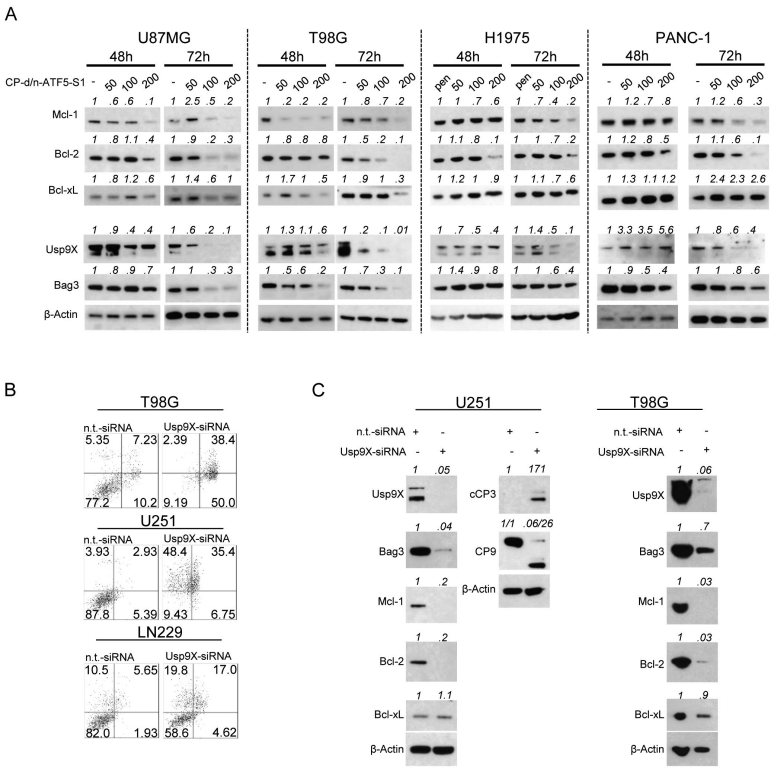

Figure 3.

A, U87MG and T98 glioblastoma as well as H1975 non-small cell lung cancer and PANC-1 pancreatic cancer cells were treated with increasing concentrations of CP-d/n-ATF5-S1 for 48h and 72h under reduced serum conditions. Whole-cell extracts were examined by Western blot for Mcl-1, Bcl-2, Bcl-xL, Usp9X and Bag3. Actin Western blot analysis was performed to confirm equal protein loading. pen indicates the usage of 100 μM Penetratin as control. Densitometric analysis was performed using ImageJ (National Institutes of Health, U.S.A., http://imagej.nih.gov/ij). *B*, T98G, U251 and LN229 glioblastoma cells were treated with non-targeting (n.t.)-siRNA or Usp9X-siRNA prior to staining with PI or annexin V/PI and flow cytometric analysis. C, T98G and U251 glioblastoma cells were treated with non-targeting (n.t.)-siRNA or Usp9X-siRNA followed by Western blot analysis for Usp9X, Bag3, Mcl-1, Bcl-2, Bcl-xL and in U251 glioblastoma cells in addition for cleaved caspase-3 (cCP3) and caspase-9 (CP9). Actin Western blot analysis was performed to confirm equal protein loading. Densitometric analysis was performed using ImageJ (National Institutes of Health, U.S.A., http://imagej.nih.gov/ij).

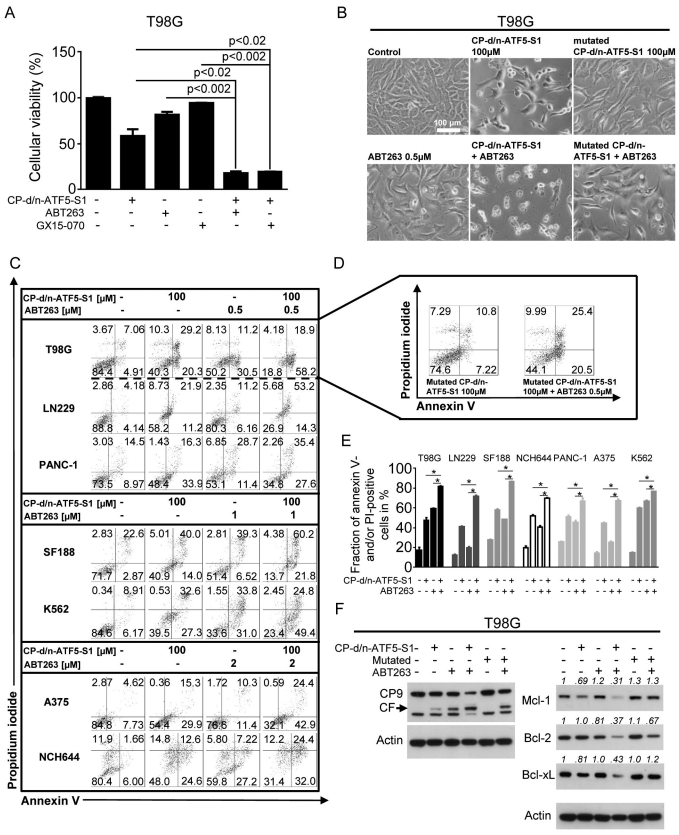

Figure 4.

A, T98G glioblastoma cells were treated for 72h under reduced serum conditions (1.5% FBS) with CP-d/n-ATF5-S1 (100 μM), ABT263 (0.5 μM) or GX15-070 (50 nM) at the indicated combinations prior to performing MTT assays. Columns: means. Error bars: standard deviation (SD). B, Representative microphotographs at 20x magnification of T98G glioblastoma cells treated with CP-d/n-ATF5-S1, ABT263, the combination of both or solvent for 48h. In addition, microphotographs of cells treated with mutated CP-d/n-ATF5-S1 alone or combined with ABT263 (0.5 μM) are shown. C, Representative flow plots of T98G, LN229, SF188 (pediatric), NCH644 (glioma stem-like) glioblastoma and PANC-1 pancreatic carcinoma, A375 melanoma, K562 chronic myeloid leukemia (in blast crisis) cells that were treated for 72h with CP-d/n-ATF5-S1 (100 μM), ABT263 (0.5 μM), the combination of both or solvent prior to staining with annexin V/propidium iodide and flowcytometric analysis. D, Representative flow plots of T98G glioblastoma cells subjected to treatment with mutated CP-d/n-ATF5-S1 alone or in combination with ABT263. E, Quantitative representation of the fraction of annexin V and/or PI-positive cells treated as described for C. * signifies a p-value of less than 0.05. Columns, means of three serial measurements. Bars, SD. F, T98G glioblastoma cells were treated with CP-d/n-ATF5-S1 (100 μM), mutated CP-d/n-ATF5-S1 (100 μM) and ABT 263 (0.5 μM) at indicated combinations for 48h under serum starvation. Whole-cell extracts were examined by Western blot for caspase-9 (CP9, CF=cleaved fragment), Mcl-1, Bcl-2 and Bcl-xL. Actin Western blot analysis was performed to confirm equal protein loading. Densitometric analysis was performed using ImageJ (National Institutes of Health, U.S.A., http://

imagej.nih.gov/ij). Data were normalized first to the respective actin control and second to the respective treatment control.

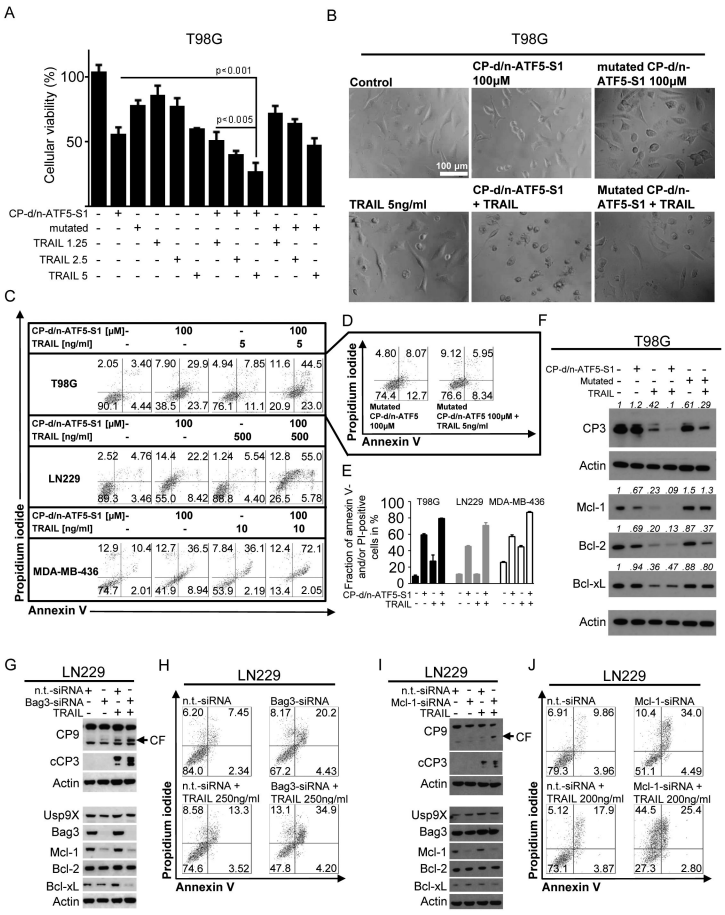

Figure 5.

A, T98G glioblastoma cells were treated with CP-d/n-ATF5-S1 (50 µM), mutated CP-d/n-ATF5-S1 (50 µM) and increasing concentrations of TRAIL as indicated. After 72h MTT assays were performed. Columns: means. Error bars: standard deviation (SD). B, representative microphotographs at 40x magnification of T98G glioblastoma cells treated with CP-d/n-ATF5-S1, TRAIL, the combination of both or solvent for 48h. In addition, microphotographs of cells treated with mutated CP-d/n-ATF5-S1 (100 µM) alone or combined with TRAIL (5 ng/ml) are shown. C, Representative flow plots of T98G, LN229 glioblastoma and MDA-MB-436 breast cancer cells treated for 72h with CP-d/n-ATF5-S1, TRAIL, the combination of both or solvent at the indicated concentrations prior to staining with annexin V/propidium iodide and flowcytometric analysis. D, Representative flow plots of T98G glioblastoma cells subjected to treatment with mutated CP-d/n-ATF5-S1 alone or in combination with TRAIL prior to staining for annexin V/PI and flowcytometric analysis. E, quantitative representation of the fraction of annexin V and/or PI-positive cells for T98G, LN229 and MDA-MB-436 cells that were treated as in C. Columns, means of three serial measurements. Bars, SD. F, T98G glioblastoma cells were treated with CP-d/n-ATF5-S1 (100 µM), mutated CP-d/n-ATF5-S1 (100 µM) and TRAIL (5 ng/ml) at indicated combinations for 24h under reduced serum conditions. Whole-cell extracts were examined by Western blot for caspase-3 (CP3), Mcl-1, Bcl-2 and Bcl-xL. Actin Western blot analysis was performed to confirm equal protein loading. Densitometric analysis was performed

using ImageJ (National Institutes of Health, U.S.A., http://imagej.nih.gov/ij). Data were normalized first to the respective actin control and second to the respective treatment control. G, LN229 glioblastoma cells were treated with non-targeting (n.t.)-siRNA, Bag3-siRNA and TRAIL as indicated. Whole-cell extracts were examined by Western blot for caspase-9 (CP9, CF=cleaved fragment), cleaved caspase-3 (cCP3), Usp9X, Bag3, Mcl-1, Bcl-2 and Bcl-xL. Actin served as loading control. H, Representative flow plots of LN229 glioblastoma cells treated with non-targeting (n.t.)-siRNA or Bag3-siRNA prior to additional treatment with TRAIL or solvent for 24h and staining with annexin V/propidium iodide plus flowcytometric analysis. I, LN229 glioblastoma cells were treated with non-targeting (n.t.)-siRNA, Mcl-1-siRNA and TRAIL as indicated. Whole-cell extracts were examined by Western blot for caspase-9 (CP9, CF=cleaved fragment), cleaved caspase-3 (cCP3), Usp9X, Bag3, Mcl-1, Bcl-2 and Bcl-xL. Actin served as loading control. J, Representative flow plots of LN229 glioblastoma cells treated with non-targeting (n.t.)-siRNA or Mcl-1-siRNA prior to additional treatment with TRAIL or solvent for 24h and staining with annexin V/propidium iodide plus flowcytometric analysis.

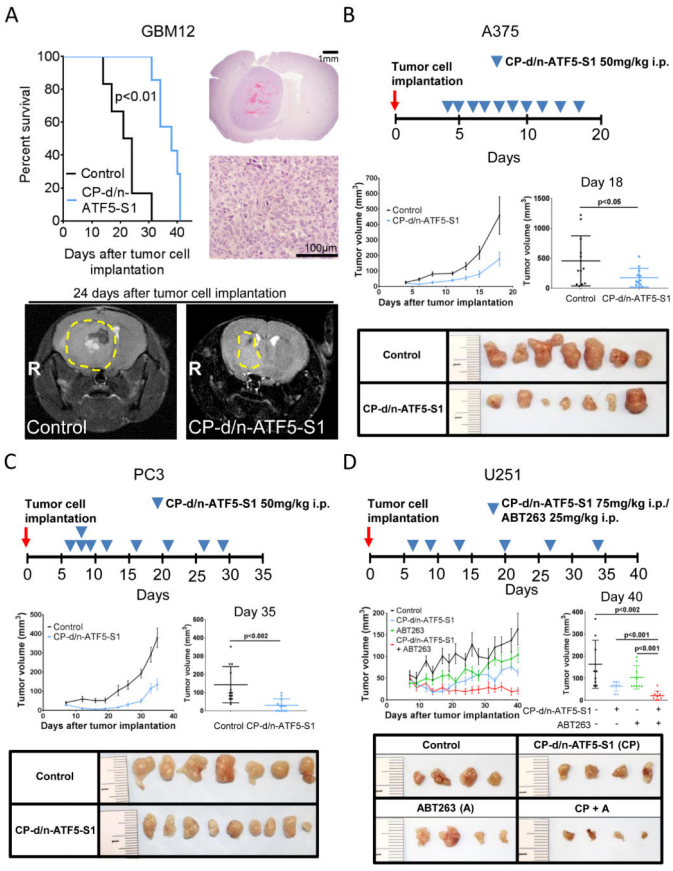

Figure 6.

A, 3×10^5 GBM12 glioblastoma cells were implanted intracranially. After tumor formation animals were treated intraperitoneally with vehicle (n=6) or CP-d/n-ATF5-S1 (n=7). Treatment was started on day 5 with a dose escalation from 50 to 150mg/kg over the first 4 days followed by a de-escalation to a maintenance therapy of 75mg/kg, 3x/week. Microphotographs at 2x and 40x magnification of a representative tumor from the vehicle-treated group are shown as well as representative brain MRIs of animals treated with vehicle or CP-d/n-ATF5-S1. B, 1×10^6 A375 malignant melanoma cells were implanted subcutaneously. After tumor formation animals were treated intraperitoneally with vehicle (n=12 tumors) or CP-d/n-ATF5-S1 (n=12 tumors) as indicated. C, 1×10^6 PC3 prostate cancer cells were implanted subcutaneously. After tumor formation animals were treated intraperitoneally with vehicle (n=12 tumors) or CP-d/n-ATF5-S1 (n=12 tumors) as indicated. D, 1×10^6 U251 glioblastoma cells were implanted subcutaneously. After tumor formation animals were treated intraperitoneally with vehicle (n=9 tumors), CP-d/n-ATF5-S1 (n=9 tumors), ABT263 (n=9 tumors) or the combination of CP-d/n-ATF5-S1 and ABT263 (n=9 tumors) as indicated. Data are presented as mean and SEM. The student's t-test was used for statistical analysis and a p-value of less than 0.05 was considered statistically significant. Representative photographs of the tumors are provided.